Effect of Erythrocyte Sedimentation and Aggregation on the Conductivity of Blood in a Miniature Chamber

Alexander Zhbanov
Department of Medical System Engineering
Gwangju Institute of Science and Technology (GIST)
Gwangju, Republic of Korea
e-mail: azhbanov@gist.ac.kr

Sung Yang
Department of Medical System Engineering
School of Information and Mechatronics
Department of Nanobio Materials and Electronics
Gwangju Institute of Science and Technology (GIST)
Gwangju, Republic of Korea
e-mail: syang@gist.ac.kr

***Abstract*—The mechanisms influencing the erythrocyte sedimentation and aggregation still remain unclear despite considerable research effort. In this study, we determined the erythrocyte sedimentation rate (ESR) by measuring the electrical conductivity of blood in a miniature chamber with two planar electrodes on the bottom. As the red blood cells settle towards the bottom, the hematocrit (HCT) or erythrocyte volume fraction increases continuously with the time in the lower part of volume. The measured conductivity of blood in the chamber slightly increased during the first minute of observation and then decreased for more than 1.5 h. The dielectric theory was applied to determine the effective conductivity of blood. We have shown the increase of blood conductivity due to aggregation by both experimentally and theoretically. We have investigated the ESR at different HCT levels by using experimentally measured decreasing of blood conductance with time. A particle dynamic model (PDM) was developed to elucidate the relationship between the microfluidic interaction of red blood cells (RBCs) and macroscopic ESR tests. We estimated the initial velocity and acceleration of erythrocytes and completion time of sedimentation.**

Keywords-blood conductivity; erythrocyte sedimentation rate (ESR); aggregation; particle dynamic model (PDM)

I. INTRODUCTION

The erythrocyte sedimentation rate (ESR) is a simple and inexpensive laboratory test for assessing the inflammatory or acute response. The International Committee for Standardization in Hematology recommends the use of the Westergren method [1]. The duration of the Westergren test is one hour. The idea of shortened erythrocyte sedimentation rate evaluation (about 30, 20, 10 min or shorter) was discussed in several works [2-4]. However, the acceleration and automation of the ESR test encounters difficulties because the mechanisms influencing the erythrocyte sedimentation rate still remain unclear, despite considerable research efforts. A critical review of current models of the erythrocyte sedimentation is given in a recent work [5].

Several investigators have measured the time dependence of the blood conductivity. These studies based on the phenomenon that, as the red cells settle, hematocrit (HCT) decreases in the upper region of the blood column [5-9]. In the present work, we study the changes in blood conductivity during the aggregation and sedimentation in a small chamber with two planar electrodes on the bottom. The measured conductance of blood in the chamber increases slightly during the first minute of observation and then decreases longer than one hour.

In this work, we try to find the relation between ESR and blood conductivity during the sedimentation. We consider the effective medium theory describing electrical conductivity of coated ellipsoidal particle suspensions. We compare our experimental data with theoretical prediction of blood conductivity. We develop a particle dynamic model (PDM) to elucidate the relationship between the microfluidic interaction of red blood cell (RBC) and macroscopic ESR test. We estimate the initial velocity and acceleration of erythrocyte and the time taken for sedimentation.

The structure of the paper is as follows. Section II describes material, methods, and measuring changes in the blood conductivity. The effective medium theory and its application to calculate the conductivity are given in Section III. The influence of RBC aggregation and sedimentation on the blood conductivity is also considered in this Section. The estimation of RBC sedimentation speed is given in Section IV. Section V offers the particle dynamic simulation of RBC aggregation and sedimentation. In addition, different ways of describing the aggregation of particles is discussed here. Our conclusions appear in Section VI.

II. CHANGES IN BLOOD CONDUCTIVITY DURING AGGREGATION AND SEDIMENTATION

A. Measurement System

The schematic drawing of fabricated device is shown in Fig. 1. The device is fabricated by conventional MEMS process. It is consists of a polydimethylsiloxane (PDMS) chamber (5mm-wide and 5mm-deep) and two gold-paleted 2D planar electrodes, each of width 300 μm with gap 1200 μm apart. The 200 nm thick gold film was sputtered and then wet etched to the shape of electrodes.

To record a data, an impedance analyzer (4294A, Agilent technologies) [10], and a data acquisition system (National Instruments, LabVIEW) [11] were used.

 ISBN: 978-1-61208-214-1

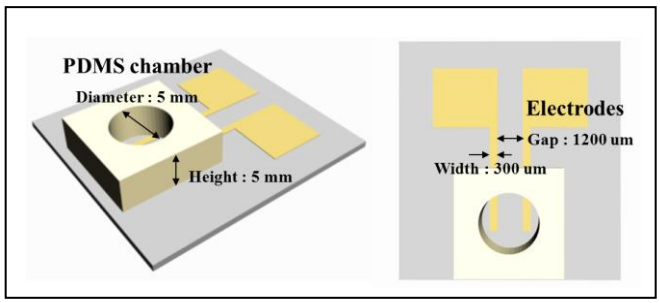

Figure 1. Schematic of the device for measuring the electrical conductivity of blood

B. *Preparation of Blood Samples*

Venous blood samples were drawn from the antecubital vein of healthy volunteers and collected in vacutainers (6 ml, BD, Franklin Lakes, NJ, USA), which contained (K2) Ethylenediaminetetraacetic acid (EDTA) as the anti-coagulant.

In order to prepare the samples with different concentrations of fibrinogen, the whole blood was centrifuged at 3000 rpm for 10 min, and then the plasma and buffy-coat were removed. The erythrocytes were washed three times with an isotonic phosphate buffered saline (PBS, pH=7.4, 290mOsmol/kg) to eliminate fibrinogen on their surface. The erythrocytes, plasma, and PBS were then mixed in desired proportion.

C. *Time Dependence of Blood Conductivity*

We measured the conductivity σ of whole blood samples, with HCT values of 35, 45, and 55%, respectively, over a period of 5000 s. The results are shown in Fig. 2. The initial change in conductivity is shown in the inset.

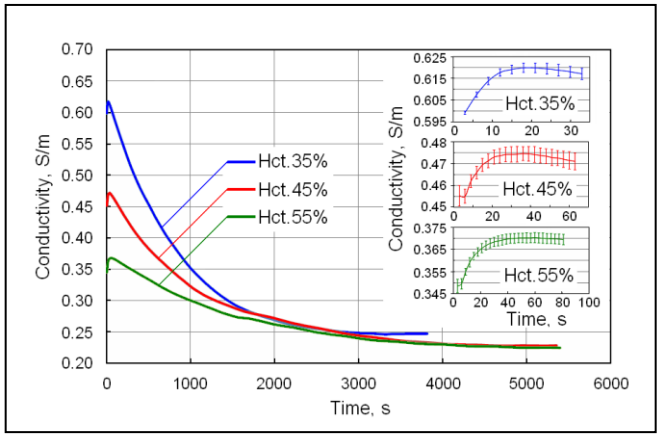

Figure 2. Changes in the conductivity of blood during sedimentation.

The effective conductivity has a physical meaning only for a homogeneous suspension of mixed particles. During sedimentation, the conductivity of blood varies on height. However, we prefer to use a unit of conductivity, because at the initial time the conductivity corresponds to the conductivity of a homogeneous blood suspension and at the end of sedimentation it is very close to the conductivity of deposit.

Fig. 2 shows that the conductivity of the blood in the chamber increased during the first minute of observation. The conductivity then decreased, and continued to do so for more than 1.5 h. The conductivity for the period during which it was increasing is shown in more detail in the inset to Fig. 2.

We injected the erythrocyte suspension into the chamber using a pipette, and immediately began recording the conductivity. In our experiments, the conductivity remained constant during the first few seconds. We attribute this to the initial movement and mixing of the suspension after it had been injected into the chamber (prior to any aggregation).

III. CONDUCTIVITY OF WHOLE BLOOD

A. *Effective Medium Theory of the Electrical Conductivity of Blood*

Erythrocytes make up ~ 99% of the total amount of cells in the blood plasma. Thus, the physical properties of red blood cells and plasma have a decisive influence on the aggregation, the sedimentation, and the electrical conductivity of blood.

The human erythrocyte is a conducting biconcave discoid coated with a thin insulating membrane. We have based our method for calculating the effective conductivity of whole blood on effective medium theory. It seems accurate to assume that blood may be considered to be a mixture of randomly oriented spheroidal particles (Fig. 3) [12, 13].

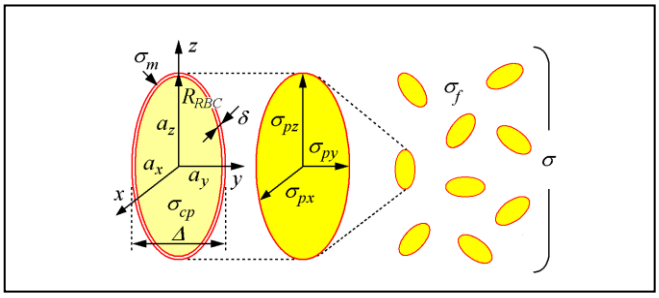

Figure 3. Model of coated spheroidal particles for red blood cells.

We define the axes of the ellipsoids to be $a_x = a_y$, and a_z (aligned with the x, y, and z axes of the reference frame), in order to model spheroidal inclusions.

The thickness δ of the erythrocyte membrane is very small (Fig. 3). In this case δ/a_x, δ/a_y, $\delta/a_z << 1$, and the volume ratio v of the inner ellipsoid to the outer ellipsoid is approximately given by

$$v \approx (1 - \delta/a_x)(1 - \delta/a_y)(1 - \delta/a_z). \quad (1)$$

The equivalent conductivity of the coated ellipsoid has three components σ_{px}, σ_{py}, and σ_{pz}. Each component σ_{pk} for the k- axis ($k = x, y, z$) is expressed as:

$$\sigma_{pk} = \sigma_m \frac{\beta_k \sigma_m + \sigma_{cp} - \beta_k \nu(\sigma_m - \sigma_{cp})}{\beta_k \sigma_m + \sigma_{cp} + \nu(\sigma_m - \sigma_{cp})}. \quad (2)$$

where σ_m and σ_{cp} are the electrical conductivity of membrane and cell cytoplasm respectively, $\beta_k = (1 - L_k)/L_k$. The depolarisation factors, L_k, in closed form are given elsewhere [12-14].

Appling Bruggeman's procedure [15] to a dispersion of ellipsoids, we can find the effective conductivity:

$$\sigma = \sigma_f + \frac{\frac{1}{3}\phi_p \sigma_f \sum_k^{x,y,z} \frac{(\sigma_{pk} - \sigma_f)}{\sigma_f + L_k(\sigma_p - \sigma_f)}}{1 + \phi_p \left[\frac{1}{3}\sigma_f \sum_k^{x,y,z} \frac{1}{\sigma_f + L_k(\sigma_{pk} - \sigma_f)} - 1 \right]}. \quad (3)$$

where σ_f is the conductivity of plasma, ϕ_p is the volume fraction of erythrocytes and σ is the conductivity of blood.

Equation (3) is similar to that proposed by Giordano et al. [16] if we use (2) for the principal conductivities.

B. Comparison of Theoretical and Experimental Data

Analyzing the published data, we selected the following average values of blood parameters: conductivity of the erythrocyte cell membrane $\sigma_m = 5 \cdot 10^{-5}$ S/m and of the RBC cytoplasm $\sigma_{cp} = 0.5$ S/m; radius of red cells $R_{RBC} = 4$ μm and thickness $\Delta = 2$ μm; membrane thickness $\delta = 7.5 \cdot 10^{-3}$ μm.

The conductivity of plasma at T = 24 and 37 °C was assumed to be $\sigma_f = 1.2$ and 1.57 S/m, respectively. All our experiments were performed at room temperature 24±1 °C. Equation (3) predicts conductivities that closely match the experimental values of the disaggregated erythrocyte suspensions.

A comparison of the blood resistivity for a range of HCT from published experimental data and our study (3) is given in Fig. 4.

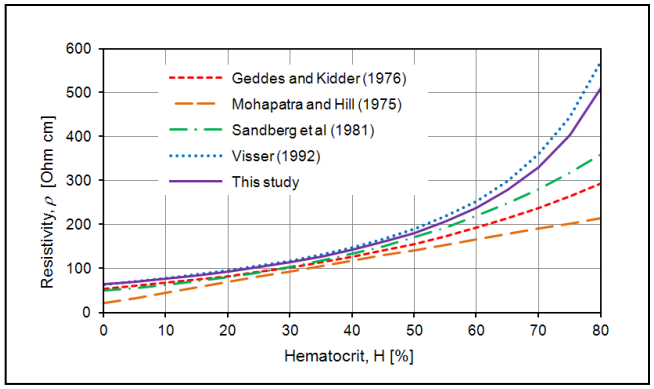

Figure 4. Dependence of the blood resistivity on HCT.

The red dotted line corresponds to Geddes and Kidder empirical formula [17]. The orange long-dashed line is Mohapatra and Hill data [18]. The green dashed-dotted line shows Sandberg et al. dependence [19]. The blue dotted line is Visser's experimental data [20]. The violet solid line shows the results generated using (3). Our approximation demonstrates a good agreement with experimental data.

C. Influence of RBC Aggregation on the Conductivity

Erythrocytes can aggregate to form rouleaux. We use the term *aggregation number* to specify the number of 'coins' in an aggregate. Fig, 5A depicts an aggregate in which the aggregation number is 5 A disaggregated mixture has aggregation number 1. A good approximation for such pile would be a heterogeneous cylinder shown in Fig. 5B. The equivalent conductivity of the heterogeneous cylinder has three components $\sigma_{px} = \sigma_{py}$, and σ_{pz} (see Fig. 5C). Applying (2) in limits when a_x and a_y tend to infinity and when a_z tends to infinity, we have $\sigma_{px} = \sigma_{py} = 0.0253$ S/m and $\sigma_{pz} = 0.00658$ S/m. Next, we use the model of prolate ellipsoids instead of cylinders (Fig. 5D).

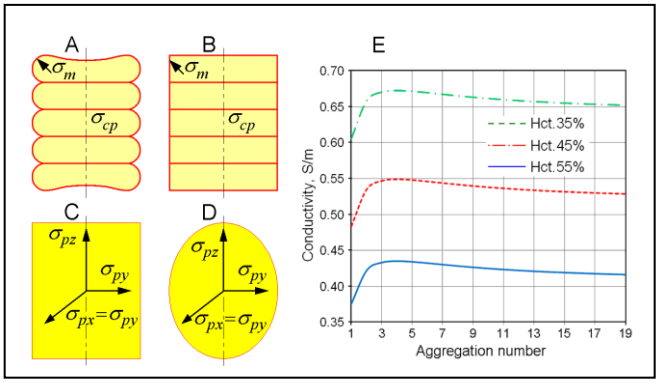

Figure 5. Models for an erythrocyte aggregation in rouleaux (A)-(D) and increasing in blood conductivity with aggregation nubmer (E).

Our calculation of changing in the whole blood conductivity with aggregation number is shown in Fig. 5E. The maximum increase in conductivity is approximately 0.075 S/m at aggregation number 4 for all levels of HCT. In our experiment we observe the maximum increase of 0.02 S/m (Fig. 2). We explain this deviation by the fact that in our experiment we have the mixture of RBCs with various aggregation numbers.

D. Decreasing of Conductivity with RBC Sedimentation

In our experiments, the conductivity approached a minimum of approximately 0.225 S/m at the end of sedimentation. Analyzing results calculated by (3) we can conclude that the HCT of deposit is H = 70%. We analytically approximated the change in conductivity with time using the following exponential dependence:

$$\sigma = A_1 \exp(-B_1 t) + C_1. \quad (4)$$

where $C_1 = 0.225$ S/m is the blood conductivity at H = 70%.

The coefficients A_1 and B_1 we obtained for different HCT are given in Table I. Equation (4) demonstrates a good agreement with experimental data.

TABLE I. COEFFICIENTS FOR THE ANALYTICAL APPROXIMATIONS

HCT	A_1, S/m	B_1, s^{-1}	A_2, S/m	B_2, $\%^{-1}$	D_2, %
35%	0.405	0.001176	0.489	0.5006	0.1409
45%	0.265	0.001005	0.325	0.5218	0.1538
55%	0.155	0.0007259	0.197	0.5622	0.1833

IV. ESTIMATION OF SEDIMENTATION SPEED

A. Model of Sedimentation

In Fig. 6A we present a simple model of a column of blood during sedimentaion. The blood column has three separate zones: the up zone of pure plasma, the middle part of initial HCT, and the deposit of hematocrit H = 70% at the bottom of column. In reality, the boundaries between zones are slightly blurred.

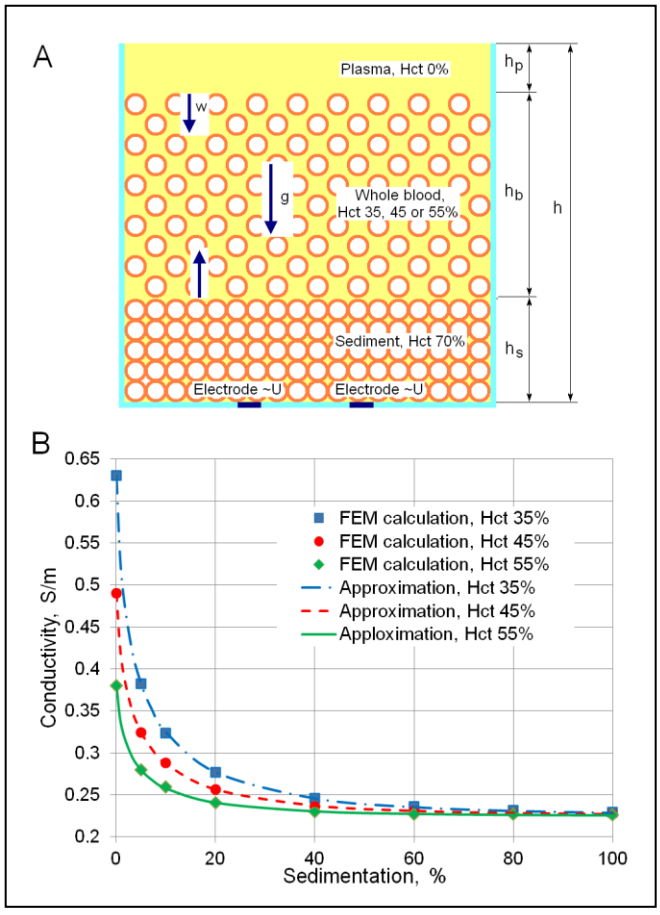

Figure 6. Simple model of RBC sedimentation (A) and approximation of conductivity dependence on sedimentation of blood (B).

We have shown that the blood conductivity only increases slightly during aggregation (see Fig. 3 and 5E). We can therefore assume that a constant electrical conductivity is maintained in the middle part of the blood column during deposition. The height of plasma zone, h_p and the height of sediment, h_s both increase, but the thickness of middle part, h_b decreases over time (Fig. 6A). The total height of the blood column is $h = h_p + h_b + h_s$. We determine the percentage of sedimentation as follows: $S = (h - h_0) / h \times 100\%$. For speed of sedimentation we use a series expansion $v = v_0 + \alpha t$, where v_0 is the initial speed of sedimentation in %/s and α is the acceleration of sedimentation in $\%/s^2$. Acceleration takes place due to aggregation, which increases the mass of the falling particles.

The time dependence of sedimentation is given by:

$$S = v_0 t + at^2/2. \quad (5)$$

The inverse relationship is

$$t = \frac{-v_0 + \sqrt{v_0^2 + 2\alpha S}}{\alpha}. \quad (6)$$

We applied a finite element simulation to calculate dependence of conductivity on sedimentation (Fig. 6B).

After substitution of (6) in (4) we have

$$\sigma(S) = A_2 \exp\left(-B_2\sqrt{D_2 + S}\right) + C_1. \quad (7)$$

where $A_2 = A_1 \exp\left(\frac{B_1 v_0}{\alpha}\right)$, $B_2 = \frac{\sqrt{2}B_1}{\sqrt{\alpha}}$, and $D_2 = \frac{v_0^2}{2\alpha}$.

We obtained the coefficients A_2, B_2, and D_2 obtained by the least square method for different HCT values; these are given in Table I. These coefficients enable the initial speed and the acceleration of sedimentation to be calculated. Their values are given in Table II. Here w_0 is the initial velocity and a is the acceleration of boundary between plasma and blood

TABLE II. INITIAL SPEED, ACCELERATION AND COMPLETION TIME OF RBC SEDIMENTATION

HCT	v_0, %/s	w_0, μm/s	α, $\%/s^2$	a, $\mu m/s^2$	t, s
35%	$1.764 \cdot 10^{-3}$	0.04409	$11.04 \cdot 10^{-6}$	$2.759 \cdot 10^{-4}$	4100
45%	$1.511 \cdot 10^{-3}$	0.02697	$7.419 \cdot 10^{-6}$	$1.325 \cdot 10^{-4}$	4993
55%	$1.106 \cdot 10^{-3}$	0.01184	$3.334 \cdot 10^{-6}$	$3.572 \cdot 10^{-5}$	7421

B. Settling Velocity

For small Reynolds number, Re < 1, the drag force of spherical particle obeys to the Stokes' law:

$$F_D = 6\pi\mu R w, \quad (8)$$

where μ is the dynamic viscosity of the fluid, R is the sphere radius, and w is the mean velocity of the sphere relative to the fluid. If the drag force equals to the gravity force and

buoyancy force, then the resulting terminal velocity, w_t is given by:

$$w_t = 2(\rho_p - \rho_f)R^2 g/9\mu. \quad (9)$$

where ρ_p and ρ_f are the densities of particle and fluid, respectively, g is the gravity acceleration.

Equation (9) indicates that particles with a greater mass will have a higher velocity. The relaxation time of a spherical particle is given by:

$$\tau = 2(\rho_p - \rho_f)R^2/9\mu. \quad (10)$$

A sphere of equivalent volume to a red cell has radius R = 2.78 μm. We can estimate the terminal velocity of individual insulated erythrocyte as w_t = 0.561 μm/s = 2.02 mm/h. The relaxation time of single erythrocyte is τ_{RBC} = 1.34 μs. This relaxation time is very short, compared to the time taken for sedimentation. We therefore conclude that RBCs have a finite initial speed.

A large number of experiments have demonstrated that a dense cloud of particles settling in a fluid has the terminal velocity lower than it is given by the Stokes' law. It has been empirically found that the reduction in terminal velocity mainly depends on the volume fraction of the particles in the system. The semi-empirical Richardson-Zaki equation [21] is one of the most commonly used correction factors:

$$w_s = w_t(1 - \phi_p)^n. \quad (11)$$

where w_s is the settling velocity at a high volumetric concentration of particles, n is an empirically determined exponent. Richardson and Zaki showed that n is a function only of the Reynolds number (in the absence of the wall effects) [21]. The empirical value for the exponent n for low Reynolds number conditions (Re < 0.2) is n = 4.65, and this is the value that we use in our analysis. Calculated settling velocity of erythrocyte sedimentation at different HCT is as follows: $w_s(0\%)$ = 0.415, $w_s(35\%)$ = 0.0599 μm/s, $w_s(45\%)$ = 0.0282, and $w_s(55\%)$ = 0.0114 μm/s. It agrees well with experimental data (see Table II).

V. PARTICLE DYNAMIC SIMULATION OF RBC AGGREGATION AND SEDIMENTATION

A. Elastic and Aggregation Forces between RBCs

Following Fenech et al. [22] we define the elastic and aggregation forces. The elastic force is given by:

$$f_e = \kappa(2R - d_{ij})^{3/2}, \text{ if } d_{ij} < 2R \text{ and 0 otherwise }, \quad (12)$$

where d_{ij} is the distance between the centers of RBCs i and j, κ is the elastic modulus.

The attractive/repulsive Morse potential is:

$$\Phi_{ij} = D\left(e^{2B(\delta_0 - \delta_{ij})} - 2e^{B(\delta_0 - \delta_{ij})}\right), \quad (13)$$

where D is the coefficient of surface energy, $\delta_{ij} = (d_{ij} - 2R)$ is the membrane cell-cell distance, δ_0 is the membrane cell-cell distance for which the attractive/repulsive force is zero.

The aggregation force can be found after differentiation of Morse potential

$$f_a = 2DAB\left(e^{2B(\delta_0 - \delta_{ij})} - e^{B(\delta_0 - \delta_{ij})}\right), \quad (14)$$

where A is the area of RBC interacting surfaces. For our simulations we used the following parameters values: κ = $1.2 \cdot 10^{-6}$ N/m; $\delta_0 = 11 \cdot 10^{-9}$ m; $B = 5 \cdot 10^6$; $DA = 5 \cdot 10^{-24}$ J [22].

For calculation of the hydrodynamic interaction forces between particles we used a method based on Stokesian Dynamics approach [23-25]. We implemented the method [24] to calculate the lubrication forces in simulations of sedimenting particles.

B. Simulation of Aggregation and Sedimentation

Fig. 7 shows the snapshots of RBC motion at first five minutes of deposition at hematocrit H = 45%. Two dimensional aggregation and sedimentation was modeled by spheres of radius R = 2.78 μm to match RBC volume.

We applied periodical boundary conditions in the particle dynamic simulation to consider the middle part of settling particles. In Fig. 7, we show the calculation only with 81 RBCs to make a clear image. The initial positions of RBCs were determined by random placing the spheres in a rectangular cell.

C. Characterization of Settling Particles

Many different ways were suggested for characterization of aggregation: AI, aggregation index; AR, aggregation radius; AAS, average aggregate size; SAF, small aggregate fraction; MAF, medium aggregate fraction; LAF, large aggregate fraction; VR, vacuum radius.

In the left panel of Fig. 7, the number of RBC in aggregate is expressed by gradation of red. The right panel of Fig. 7 indicates the number of neighbours connected with the erythrocyte. The empty circle represents an individual erythrocyte. Yellow, orange, red, and reddish-brown circles indicate that cell is surrounded by 1, 2, 3, and 4 neighbours, respectively. Changes of VR are also given in Fig. 7.

The increase in the average settling velocity at different HCT with time is shown in Fig. 8. One can see a good agreement between calculated and experimental data.

 ISBN: 978-1-61208-214-1

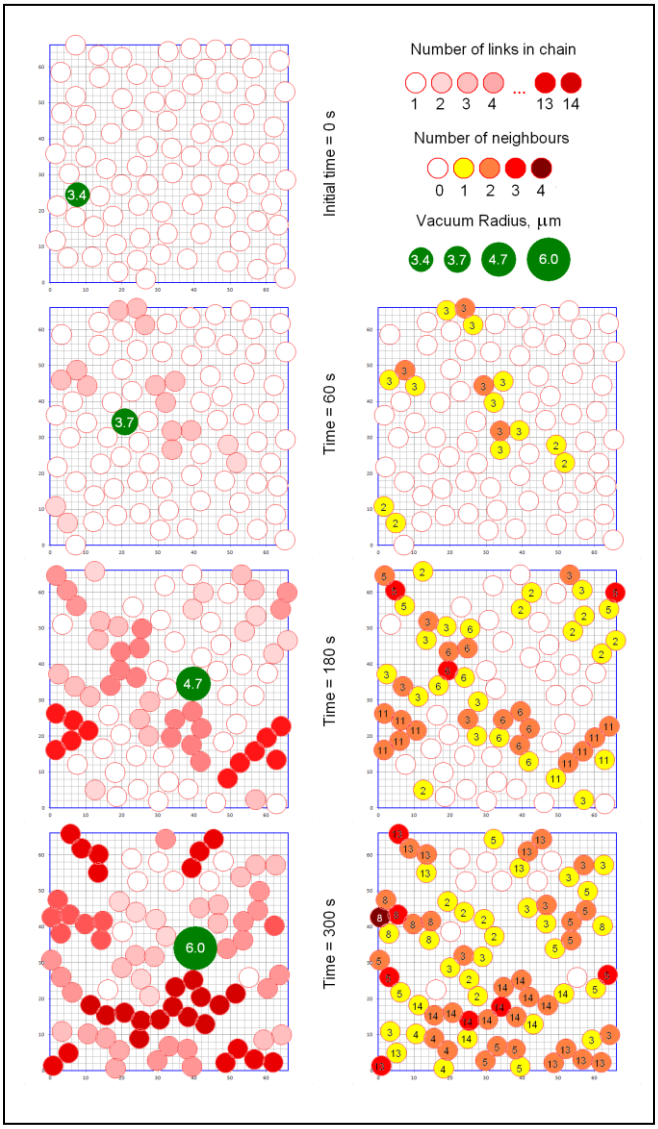

Figure 7. Snapshots of sedimentation and aggregation.

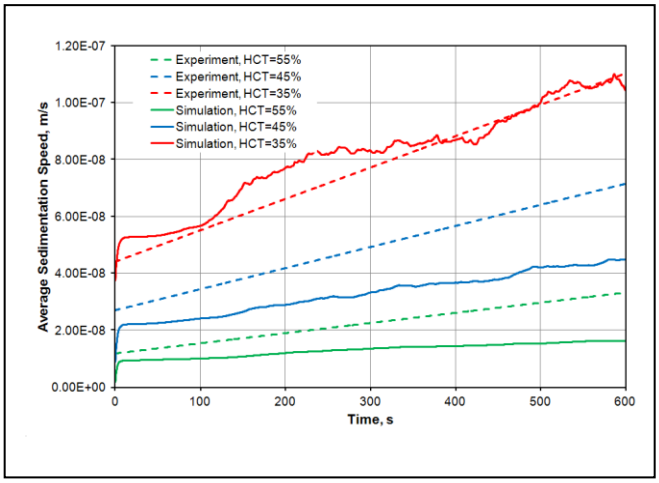

Figure 8. Changes of RBC settling velocity with time.

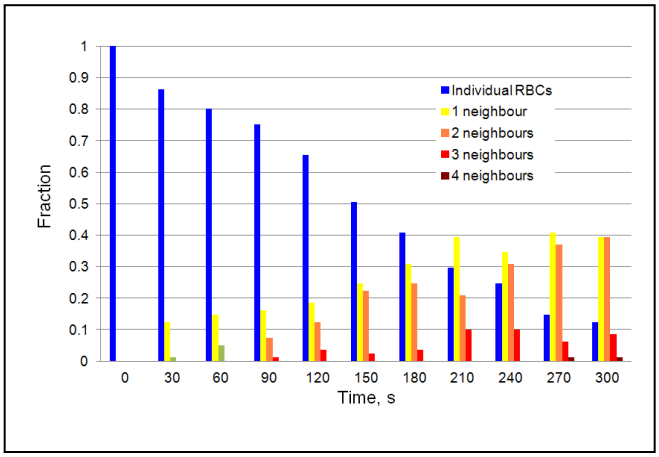

Figure 9. Fraction of particles surrounded by neighbours.

The change in velocity over time is largely dependent on the initial distribution of particles in the computational cell, but on average corresponds to uniformly accelerated motion.

We believe that an important characteristic of the aggregation and sedimentation is the fraction of particles surrounded by different number of neighbours (Fig. 9). We assume that acceleration of settling velocity takes place due to aggregation, which increases the mass of the falling particles.

By comparing Fig. 8 with Fig. 9, it clearly shows that the settling velocity and the number of aggregated particles are strongly related.

Analysis of the simulation also shows that some particles sometimes rise up. We observed the formation and collapse of a RBC networks. The sedimentation rate demonstrates a complex stochastic behavior in time.

VI. CONCLUSION

We studied the changes in blood conductivity during aggregation and sedimentation in a miniature chamber with two planar electrodes on the bottom. The dielectric theory was applied to determine the conductivity of the whole blood. The erythrocytes were modeled as conducting oblate spheroid coated with a thin insulating membrane. The conductivity of erythrocyte rouleaux formations was described by prolate spheroids with different components of conductivity. The experimentally measured conductance of blood in the chamber slightly increases during the first minute of observation and then decreases for more than 1.5 h. We attribute the slight increase in blood conductivity within the first minute to erythrocyte aggregation. Our theoretical calculations predict increase in conductivity with the number of erythrocytes aggregated. The calculation results are in good agreement with experiment. Further

 ISBN: 978-1-61208-214-1

decrease in electrical conductivity is caused by deposition of red cells at the bottom of chamber. We analytically approximated the change in the blood conductivity on time and dependence between conductivity and sedimentation. Using these approximations we estimated the initial velocity and acceleration of erythrocyte sedimentation. A particle dynamic model was developed to investigate the microfluidic RBC interaction. We estimated the initial velocity and acceleration of erythrocytes and completion time of sedimentation. As a result, the relation between the ESR and the blood conductivity was found. It is likely that our method could also be applied to accelerated ESR tests.

ACKNOWLEDGMENT

This work was partially funded by grants from the Ministry of Education, Science and Technology (MEST, KRF-20110028861), World Class University Program (R31-2008-000-10026-0) and the institute of Medical System Engineering (*iMSE*), GIST, Republic of Korea.

REFERENCES

[1] J. M. Jou, S. M. Lewis, C. Briggs, S. H. Lee, B. De La Salle, and S. McFadden, "ICSH review of the measurement of the erythocyte sedimentation rate," Int. J. Lab. Hematol., vol. 33, April 2011, pp. 125-132, doi:10.1111/j.1751-553X.2011.01302.x.

[2] P. Yagupsky and J. E. Bearman, "Shortened erythrocyte sedimentation rate,".Pediatr. Infect. Dis. J., vol. 6, May 1987, pp. 494-495.

[3] T. Alexy, E. Pais, and H. J. Meiselman, "A rapid method to estimate Westergren sedimentation rates," Rev. Sci. Instrum., vol. 80, Sep. 2009, Vol. 80, pp. 096102 (3 pages).

[4] M. Shteinshnaider, D. Almoznino-Sarafian, I. Tzur, S. Berman, N. Cohen, and O. Gorelik, "Shortened erythrocyte sedimentation rate evaluation is applicable to hospitalised patients," Eur. J. Intern. Med., vol. 21, Jun. 2010, pp. 226-229, doi:10.1016/j.ejim.2010.02.002.

[5] A. Pribush, D. Meyerstein, and N. Meyerstein, "The mechanism of erythrocyte sedimentation. Part 1: Channeling in sedimenting blood," Colloid. Surf. B-Biointerfaces, vol. 75, Jan. 2010, pp. 214-223, doi:10.1016/j.colsurfb.2009.08.036.

[6] K. Cha, E. F. Brown, and D. W. Wilmore, "A new bioelectrical impedance method for measurement of the erythrocyte sedimentation rate," Physiol. Meas., vol. 15, Nov. 1994, pp. 499-508, doi:10.1088/0967-3334/15/4/011.

[7] A. Pribush, D. Meyerstein, and N. Meyerstein, "The mechanism of erythrocyte sedimentation. Part 2: The global collapse of settling erythrocyte network," Colloid. Surf. B-Biointerfaces, vol. 75, Jan. 2010, P. 224-229, doi:10.1016/j.colsurfb.2009.08.037.

[8] A. Pribush, L. Hatskelzon, and N. Meyerstein, "A novel approach for assessments of erythrocyte sedimentation rate," Int. J. Lab. Hematol., vol. 33, Jun. 2011, pp. 251-257, doi:10.1111/j.1751-553X.2010.01277.x.

[9] A. Pribush, D. Meyerstein, and N. Meyerstein, "The effect of the prior flow velocity on the structural organization of aggregated erythrocytes in the quiescent blood," Colloid. Surf. B-Biointerfaces, vol. 82, Feb. 2011, pp. 518-525 , doi:10.1016/j.colsurfb.2010.10.010.

[10] http://www.home.agilent.com/agilent/home.jspx

[11] http://www.ni.com/labview/

[12] K. Asami and T. Yonezawa, "Dielectric behavior of non-spherical cells in culture," Biochim. Biophys. Acta, vol. 1245, Dec. 1995, pp. 317-324, doi:10.1016/0304-4165(95)00116-6.

[13] K. Asami, "Characterization of heterogeneous systems by dielectric spectroscopy," Prog. Polym. Sci., vol. 27, Oct. 2002, pp. 1617-1659. doi:10.1016/S0079-6700(02)00015-1.

[14] S. Giordano, "Effective medium theory for dispersions of dielectric ellipsoids," Electrostat., vol. 58, May 2003, pp. 59-76, doi:0.1016/S0304-3886(02)00199-7.

[15] D. A. G. Bruggeman, "Berechnung verschiedener physikalischer Konstanten von heterogenen Substanzen. I. Dielektrizitätskonstanten und Leitfähigkeiten der Mischkörper aus isotropen Substanzen," Ann. Phys.-Berlin, vol. 416, Jul. 1935, pp. 636-664, doi:10.1002/andp.19354160705.

[16] S. Giordano, P. L. Palla, and L. Colombo, "Effective permittivity of materials containing graded ellipsoidal inclusions," Eur. Phys. J. B, vol. 66, Jan. 2008, pp. 29-35, doi:10.1140/epjb/e2008-00382-7.

[17] L. A. Geddes and H. Kidder, "Specific resistance of blood at body temperature II," Med. Biol. Eng. Comput., vol. 14, Mar. 1976, pp. 180-185, doi:10.1007/BF02478745.

[18] S. N. Mohapatra and D. W. Hill, "The Changes in Blood Resistivity with Haematocrit and Temperature," Intensive Care Med., vol. 1, Dec. 1975, pp. 153-162, doi:10.1007/BF00624433.

[19] K. Sandberg, B. A. Sjöqvist, and T. Olsson, "Relation between Blood Resistivity and Hematocrit in Fresh Human Fetal Blood," Pediatr. Res., vol. 15, Jun. 1981, pp. 964-966, doi:10.1203/00006450-198106000-00017.

[20] K.B. Visser, "Electric conductivity of stationary and flowing human blood at low frequencies," Medical and Biological Engineering and Computing, vol. 30, Nov. 1992, pp. 636-640, doi:10.1007/BF02446796.

[21] J. F. Richardson and W.N. Zaki, "Sedimentation and fluidisation: Part I," Trans. Inst. Chem. Engs., vol. 32, 1954, pp. 35-53.

[22] M. Fenech, D. Garcia, H. J. Meiselman, and G. Cloutier, "A particle dynamic model of red blood cell aggregation kinetics," Ann. Biomed. Eng., vol. 37, Nov. 2009, pp. 2299-2309, doi:10.1007/s10439-009-9775-1.

[23] T. Kumagai, "Numerical analysis of equation of motion for a cluster of spheres in fluid at low Reynolds numbers," JSME J. Ser. B, vol. 38, Apr. 1995, pp. 563-569, doi:10.1299/jsmeb.38.563.

[24] C. Vanroyen, A. Omari, J. Toutain, and D. Reungoat, "Interactions between hard spheres sedimenting at low Reynolds number," Eur. J. Mech. B-Fluids, vol. 24, Sep.-Oct. 2005, pp. 586-595, doi:10.1016/j.euromechflu.2005.01.002.

[25] G. C. Abade and F. R. Cunha, "Computer simulation of particle aggregates during sedimentation," Comput. Meth. Appl. Mech. Eng., vol. 196, nos. 45-48, Sep. 2007, pp. 4597-4612, doi:10.1016/j.cma.2007.05.022

 ISBN: 978-1-61208-214-1